

See discussions, stats, and author profiles for this publication at: <https://www.researchgate.net/publication/338064707>

Evolution of cooperation in populations with heterogeneous multiplicative resource dynamics

Preprint · December 2019

CITATIONS

0

READS

101

5 authors, including:



Viktor Stojkoski

Ss. Cyril and Methodius University in Skopje

71 PUBLICATIONS 444 CITATIONS

SEE PROFILE



Marko Karbevski

Polar Cape

4 PUBLICATIONS 10 CITATIONS

SEE PROFILE



Zoran Utkovski

University Carlos III de Madrid

88 PUBLICATIONS 511 CITATIONS

SEE PROFILE



Lasko Basnarkov

Ss. Cyril and Methodius University in Skopje

57 PUBLICATIONS 336 CITATIONS

SEE PROFILE

Some of the authors of this publication are also working on these related projects:



“Innovative cooperation initiatives in cross-border region” - INTERREG- IPA CBC CCI Number 2014TC16I5CB006. [View project](#)



cooperation on graphs through generalized reciprocity [View project](#)

Evolution of cooperation in populations with heterogeneous multiplicative resource dynamics

Viktor Stojkoski¹, Marko Karbevski^{1,2,3}, Zoran
Utkovski⁴, Lasko Basnarkov^{1,5}, and Ljupco Kocarev^{1,5}

¹*Macedonian Academy of Sciences and Arts,
P.O. Box 428, 1000 Skopje, Republic of Macedonia*

²*Sorsix International, Dame Gruev 18,
Skopje 1000, Republic of Macedonia*

³*Institute of Mathematics, Faculty of Natural Sciences and Mathematics,
Ss. Cyril and Methodius University,
Arhimedova 3, 1000 Skopje, Republic of Macedonia*

⁴*Fraunhofer Heinrich Hertz Institute,
Einsteinufer 37, 10587, Berlin, Germany and*

⁵*Faculty of Computer Science and Engineering,
Ss. Cyril and Methodius University,
P.O. Box 393, 1000 Skopje,
Republic of Macedonia*

(Dated: December 20, 2019)

Abstract

In the pooling and sharing mechanism of multiplicatively grown individual resources, the evolution of cooperation is uniquely determined by the physical traits of the population. If the entities in the population exhibit homogeneous traits, cooperation is always favored. However, if there is heterogeneity within the population, the evolution of cooperation is dependent on both the interaction structure and the decision making rules implemented by the entities. Here, we perform a detailed analysis on the role of the interaction structures in the evolutionary stability of cooperation in heterogeneous multiplicative environments. We utilize this analysis to examine the applicability of a simple state-based decision making rule in a variety of settings. We thereby show that the introduced rule leads to steady state cooperative behavior that is always greater than or equal to the one predicted by evolutionary stability analysis and discuss relevant implications to natural and artificial systems.

I. INTRODUCTION

Cooperation is observed when a group of individual entities sacrifice their own resources as a means to achieve a collective gain. Despite an abundance of both empirical and theoretical studies, the appealing explanation for the evolution and stability of this behavior is still regarded as one of the most challenging issues that need to be resolved in the near future [1].

One intuitive factor that crucially determines the evolution of cooperative behavior is the dynamics which regulate the growth of resources owned by an individual entity [2]. Traditional game theory has predominantly focused on additive settings, mainly due to the difficulty in analyzing various dynamical structures. This leads to the world of two-player iterative social dilemmas where we encounter situations such as the iterated prisoner's dilemma, or multi-player (i.e. public goods) games [3]. It is widely acknowledged that under such circumstance, cooperation cannot evolve by itself as the dominant trait within a population. Instead, the emergence of cooperation is conditioned on the presence of other mechanisms such as kin selection, reciprocity and even topological (network) structures [4].

More complex, multiplicative dynamics that are ubiquitous in nature have received much less attention by the scientific community [5]. Only recently it has been shown that under such dynamics the evolution of cooperation may not be dependent on any auxiliary mechanisms. In particular, in a simple setting where individual entities with homogeneous physical characteristics are able to pool and share their multiplicatively grown resources, cooperation is the sole evolutionary stable strategy [6–8]. When the homogeneity assumption is relaxed, complex behavior occurs and the stability of cooperation is dependent on both the interaction structure and the decision making rules employed by the entities [8]. Nevertheless, the role of these two mechanisms in the cooperative dynamics where the resources of individual entities undergoes a multiplicative process remains largely unexplored.

A. Our contribution

To provide a better understanding of the extent to which interaction structures and decision making rules promote cooperation under multiplicative resource dynamics, here we revisit the model of networked Geometric Brownian motion (GBM) and generalize it to account for possible heterogeneous traits within the population [9]. The networked GBM

is a simple model in which the dynamics of the log of resources undergoes a Brownian motion. Cooperation is introduced in this model by discretizing the process and allowing each individual entity to pool its resources at the end of each growth phase, and afterwards the pooled resources are shared. The way in which individuals interact in the resulting pooling and sharing mechanism is determined by a predefined complex network structure.

By analyzing the model from an evolutionary perspective, we derive the criteria required for cooperation to be stable within any interaction structure. More importantly, by applying these criteria to simple tractable, as well as complex numerical examples, we are able to show that the interaction structure may non-linearly affect the behavior in multiplicative dynamics. This leads to creation of cooperative components. Each component is characterized with essentially different evolutionary properties. In particular, entities within different components may co-evolve even though the resources owned by one of them are negligible in comparison to those of the others.

The evolutionary stability analysis assumes that each individual entity behaves either as an unconditional defector (i.e. it never cooperates), or as an unconditional cooperator (always cooperates). As such it does not allow us to examine the effect of the decision making rules employed by the individual entities. Due to the non-ergodicity arising as a consequence of the multiplicative environment, standard rules such as direct or indirect reciprocity cannot be easily translated to our model [10]. Instead, one should use a suitable modification of the rule which is studied.

To shed valuable insight on the impact of such rules, here we develop a simple behavioral update dependent only on the observed growth of the resources owned by an individual entity and examine its implications. The introduced rule is simple and is directly related to the concept of generalized reciprocity, which itself is rooted in the principle of “help anyone if helped by someone” [11]. We thereby show that our rule leads to steady state cooperative behavior that is always greater than or equal to the one predicted by evolutionary stability analysis. In fact, for a certain regime of parameter values we are able to analytically solve the model and show that then the strict inequality holds. Direct parallels can be made to state-of-the-art reinforcement learning techniques based on novelty search [12].

The rest of the paper is organized as follows. Section II is concerned with putting the theoretical model in context, and a brief summary on the properties of pooling and sharing in

networked GBM with heterogeneous drifts and amplitudes is given. In Section III we study the model from an evolutionary biology point of view and derive the criteria required for a given complex network to be evolutionary stable. Here, we also solve several analytically tractable examples that elucidate the role of the network structure and examine numerically the extent to which different complex network topologies promote cooperative behavior. In Section IV we discuss the concept of generalized reciprocity, introduce our decision making rule and study its properties. The last section briefly summarizes our findings.

II. MODEL

A. Interaction structure

We assume a system constructed of a population of N individual entities interacting through M pools. The interaction structure is described by a connected bipartite random graph, whose adjacency matrix \mathbf{B} with binary edge variables $B_{im} \in \{0, 1\}$ captures the participation of individual i in pool m ($B_{im} = 1$, indicating participation of i in pool m).

The main advantage of modeling through bipartite networks instead of standard monopartite, is that they offer a more coherent depiction for the composition of groups and spread of information within the population [13]. In addition, this representation allows for a direct comparison with standard multi-player games with additive dynamics played on networks, as will be seen in the following.

The dynamics of the system, which runs in discrete time and explains the evolution of the resource endowment $y_i(t)$ of each individual entity i in \mathcal{N} , can be described as follows. First, at every period the resources of each entity grow multiplicatively with a fluctuating rate that has a drift μ_i and a noise amplitude σ_i . Next comes a pooling phase where each entity i distributes a fraction $p_i(t)/d_i$ of its resources to each of the d_i pools it belongs to. Finally, every pool shares a fraction d_m of the total pooled resources to each of its members. Mathematically, the dynamics can be expressed as

$$y_i(t + \Delta t) = \underbrace{\sum_j A_{ij} p_j(t) y_j(t) \left[1 + \mu_j \Delta t + \sigma_j \varepsilon_j(t) \sqrt{\Delta t} \right]}_{\text{resources due to pooling and sharing}} + \underbrace{(1 - p_i(t)) y_i(t) \left[1 + \mu_i \Delta t + \sigma_i \varepsilon_i(t) \sqrt{\Delta t} \right]}_{\text{individual resources}}, \quad (1)$$

where $\varepsilon_j(t)$ is a standardized Gaussian random variable and \mathbf{A} is a transition matrix of the network with entries $A_{ij} = \sum_m^M \frac{B_{im}}{d_m} \frac{B_{jm}}{d_j}$ which determine the total allocated resources from entity j to entity i . The variable $p_i(t) \in [0, 1]$ models the level of cooperation displayed by an individual entity in a particular period as it represents the incentive of that entity to pool and share its resources.

By setting $\Delta t \rightarrow 0$, we can write Eq. (1) in a differential form as

$$dy_i = \left[\sum_j A_{ij} p_j y_j - p_i y_i \right] dt + \sum_j A_{ij} p_j y_j (\mu_j dt + \sigma_j dW_j) + (1 - p_i) y_i (\mu_i dt + \sigma_i dW_i), \quad (2)$$

where $(dW_i)_{i \in \mathcal{N}}$ are independent Wiener increments, i.e. $W_i(t) = \int_0^t dW_i$.

The resulting interaction structure is directly related to games of public goods on networks with the main difference that in this model the noise comes inherently from the individual traits within the entities instead of an aggregate pool stochasticity [3, 13, 14].

B. Growth rate

When the steady state incentive for cooperation by each entity i is $p_i^* = 0$, we have the unconditional defector situation and the model reduces to N independent geometric Brownian motion (GBM) trajectories. The multiplicative nature of GBM makes the process non-stationary, and hence non-ergodic. This implies that ensemble and time-average behavior will differ and therefore we can not simply use $y_i(t)$ as a measure for the evolutionary performance of one entity. Instead, a suitable ergodic transformation of this observable should be utilized.

For this purpose we resort to the time-average growth rate $g_i(y_i(t), t)$. This observable has been widely used for quantifying the performance of an entity interacting in a multiplicative environment. In particular, in evolutionary biology, the time-average growth rate is widely acknowledged as the geometric mean fitness for the accumulated payoff (i.e. resources) of a particular phenotype [15]. Formally, it is defined as

$$g_i(y_i(t), t) = \frac{1}{t} \log \left(\frac{y_i(t)}{y_i(0)} \right), \quad (3)$$

where $y_i(0)$ is the initial amount of resources. For simplicity, we are always going to assume that $y_i(0) = 1$.

In an independent GBM trajectory the steady state time-average growth rate can be easily found using Itô calculus as

$$g_i^{\mathcal{D}} = \lim_{t \rightarrow \infty} g_i^{\mathcal{D}}(y_i(t), t) = \mu_i - \frac{\sigma_i^2}{2}, \quad (4)$$

where the superscript \mathcal{D} denotes the case where no individual entity pools its resources.

On the other hand, when every entity cooperates unconditionally, i.e. $p_i(t) = 1$ for all i and t , the growth rate of each entity converges to the same value,

$$g^{\mathcal{C}} = \lim_{t \rightarrow \infty} g_i(y_i(t), t) = \langle \mu v \rangle_{\mathcal{N}} - \frac{1}{2N} \langle v^2 \sigma^2 \rangle_{\mathcal{N}}, \quad (5)$$

where the superscript \mathcal{N} denotes that every entity pools its resources, $\langle \cdot \rangle_{\mathcal{N}}$ is the population average and v is an index represented by the right-eigenvector associated with the largest eigenvalue of \mathbf{A} normalized in a way such that $\sum_i v_i = N$. For the derivation see [9].

III. EVOLUTIONARY STABILITY

A. Preliminaries

We begin the analysis by considering the circumstance in which every individual entity can behave either as an unconditional cooperator ($p_i(t) = p_i^* = 1$ for all t) or an unconditional defector ($p_i(t) = p_i^* = 0$ for all t) and examine the Evolutionary Stable State (ESS). As discussed in Nowak [4], an ESS is a situation where a large population of cooperators cannot be invaded by defectors under deterministic selection dynamics and has been widely used for determining the level of cooperative behavior in various interaction structures [16].

Notably, in a simple interaction structure consisting of two entities i and j , the possible outcomes are described with a payoff matrix

$$\begin{array}{cc}
 & \begin{array}{c} j \\ C \quad D \end{array} \\
 \begin{array}{c} i \\ C \\ D \end{array} & \begin{array}{|c|c|} \hline \pi_{CC} & \pi_{CD} \\ \hline \pi_{DC} & \pi_{DD} \\ \hline \end{array}
 \end{array} \quad (6)$$

where π_{ab} denotes the payoff of entity i under strategy a when entity j has chosen strategy b . Obviously, in our case, the strategies translate to either being a unconditional cooperator C or

defector D and the payoffs to the growth rates of the entities. This implies that cooperation is ESS if $\pi_{CC} > \pi_{DC}$. In interaction structures involving multiple entities cooperation is ESS if the overall gain for an individual entity of cooperating is greater than the situation when behaves as a defector, assuming that all other individuals cooperate unconditionally. This implies, that in the networked pooling and sharing mechanism full cooperation will be ESS if

$$g^C > \max_i g_i^D.$$

B. Growth rate

In a more general setting, cooperation may only be favored by a certain subset \mathcal{C}_l of the population whereas for the other part it is optimal to behave as unconditional defectors. This intermediate case leads to emergence of connected components where each component has its own growth rate depending on the network parameters.

To provide a better intuition on this behavior, in Fig. 1 we illustrate three situations which lead to different growth rate outcomes by considering a simple network composed of five entities and two pools. In particular, in Fig. 1a we assume that cooperation is evolutionary stable for all entities, Therefore, in this case the growth rate of each individual entity converges to (8). On the other hand, in, Fig. 1b we set the growth rate of entity 3, which acts as bridge by being the only one to pool its resources in both pools, to be large enough so as this entity behaves as an unconditional defector. This creates two separate components $\mathcal{C}_1 = \{1, 2\}$ and $\mathcal{C}_2 = \{4, 5\}$, which pool and share resources only between themselves. Notice that the entities also pool part of their resources to entity 3 but they are not shared back. This implies that the resource dynamics, and hence growth rates, between the components are independent. If the growth rates of each component are different, this leads to great discrepancies in the observed resources between the cooperators belonging to separate components, with the resources of the entities in one component being negligible in comparison to the resources of the entities in the other component. Finally, in the last example, besides entity 3 we also set the entities in component \mathcal{C}_2 to be defectors. Thus, in this case each cooperator will have the same steady state growth rate.

To analyze the steady state growth rate g_i^* of the entities in component \mathcal{C}_l we utilize a

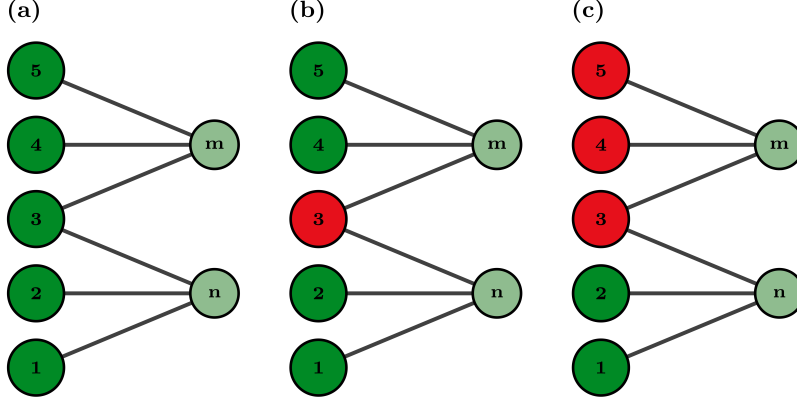


FIG. 1: **Creation of cooperative components.** (a-c) Network composed of five entities. Green nodes are the entities which prefer cooperation, whereas the red nodes depict entities which favor defection.

mean-field approach together with Itô calculus, as is done in [9]. The mean-field approach assures that each connected component of cooperators \mathcal{C}_i will have a convergent growth rate given by the growth rate of the average $\langle y \rangle_{\mathcal{C}_i}$ constructed by the resource trajectories of the entities belonging to this component.

To prove this claim, we define the rescaled resources of each cooperating entity i as $\hat{y}_i(t) = \frac{y_i(t)}{\langle y \rangle_{\mathcal{C}_i}}$. Due to the normalization, in steady state, this observable also converges to a constant value \hat{y}_i^* that is greater than zero and less than the number of cooperators. Hence, the growth rate of each entity i in the set of cooperators can be written as

$$\begin{aligned}
 \lim_{t \rightarrow \infty} g_i(y_i(t), t) &= \lim_{t \rightarrow \infty} \frac{1}{t} \log \left(\frac{y_i(t)}{y_i(0)} \right) \\
 &= \lim_{t \rightarrow \infty} \frac{1}{t} \log (\langle y(t) \rangle_{\mathcal{C}_i} \cdot \hat{y}_i(t)) \\
 &= \lim_{t \rightarrow \infty} \frac{1}{t} \log (\langle y(t) \rangle_{\mathcal{C}_i}) + \lim_{t \rightarrow \infty} \frac{1}{t} \log (\hat{y}_i(t)) \\
 &= \lim_{t \rightarrow \infty} \frac{1}{t} \log (\langle y(t) \rangle_{\mathcal{C}_i}) \\
 &\doteq \lim_{t \rightarrow \infty} g(\langle y(t) \rangle_{\mathcal{C}_i}, t).
 \end{aligned}$$

Consequently, one can use Itô's lemma to directly calculate the cooperative time-average growth rate. Formally, the lemma states that the differential of an arbitrary one-dimensional

function $f(\mathbf{y}, t)$ governed by an Itô drift-diffusion process is given by

$$df(\mathbf{y}, t) = \frac{\partial f}{\partial t} dt + \sum_i \frac{\partial f}{\partial y_i} dy_i + \frac{1}{2} \sum_i \sum_j \frac{\partial^2 f}{\partial y_i \partial y_j} dy_i dy_j. \quad (7)$$

In the case of $g(\langle y \rangle_{C_l}, t)$, we have that $f(t, \mathbf{y}) = \log(\langle y \rangle_{C_l})$. Then, the first and second derivative of f with respect to y_i and y_j are easily calculated as $\frac{\partial f}{\partial y_i} = \frac{1}{N_{C_l}} \frac{1}{\langle y \rangle_{C_l}}$ and $\frac{\partial^2 f}{\partial y_i \partial y_j} = -\frac{1}{N_{C_l}^2} \frac{1}{\langle y \rangle_{C_l}^2}$, where N_{C_l} is the number of cooperators in steady state. Moreover, this transformation makes the differential $df(\mathbf{y}, t)$ ergodic, and since we are looking at steady state averages, dy_i and $dy_i dy_j$ can be substituted with their expected values $\langle dy_i \rangle$ and $\langle dy_i dy_j \rangle$. To estimate these expectations we utilize the independent Wiener increment property $\langle dW_i^2 \rangle = dt$, and define $z_j^{[C_l]} = \sum_{k \in C_l} A_{kj}$. Further, we omit terms of order dt^2 as they are negligible. As a result, we obtain that

$$\langle dy_i \rangle = \left[\sum_{k \in C_l} A_{ik} (1 + \mu_k) y_k - y_i \right] dt,$$

and,

$$\langle dy_i dy_j \rangle = \sum_{k \in C_l} A_{ik} A_{jk} \sigma_k^2 y_k^2 dt.$$

By inserting the estimates in equation (7) we can approximate the time-average growth rate as

$$g(\langle y \rangle_{C_l}, t) = \frac{1}{N_{C_l}} \sum_{i \in N_{C_l}} \hat{y}_i(t) \left[(1 + \mu_i) z_i^{[C_l]} - 1 \right] - \frac{1}{2} \frac{1}{N_{C_l}^2} \sum_{i \in C_l} (z_i^{[C_l]} \hat{y}_i(t))^2 \sigma_i^2. \quad (8)$$

Equation (8) describes the growth of $\langle y \rangle_{C_l}$ as a function of $\hat{y}_i(t)$. To derive its steady state behavior, notice that we can neglect the defectors from the cooperative dynamics and rewrite Eq. (1) as

$$y_i(t + \Delta t) = \sum_{j \in C_l} A_{ij} y_j(t) \left[1 + \mu_j \Delta t + \sigma_j \varepsilon_j(t) \sqrt{\Delta t} \right]. \quad (9)$$

When equation (9) is divided by the population average resources $\langle y(t + \Delta t) \rangle_{C_l}$ and is written in matrix form, the steady state dynamics for the rescaled resources can be approximated as

$$\hat{\mathbf{y}}^* = \lim_{t \rightarrow \infty} \hat{\mathbf{y}}(t) \approx \lim_{t \rightarrow \infty} \frac{\mathbf{A}_{C_l} \mathbf{y}(t)}{\langle \mathbf{A}_{C_l} \mathbf{y}(t) \rangle_{C_l}}, \quad (10)$$

where $\mathbf{A}_{\mathcal{C}_l}$ is a reduced version of the transition matrix \mathbf{A} in which includes only the rows and columns associated to the individuals in the set \mathcal{C}_l . By the power method, this leads to

$$\hat{y}_i^* = v_i^{[\mathcal{C}_l]}, \quad (11)$$

where $v_i^{[\mathcal{C}_l]}$ is the i -th element of the right-eigenvector of $\mathbf{A}_{\mathcal{C}_l}$ associated with the largest eigenvalue $\lambda_{\mathcal{C}_l}$ normalized in a way such that $\sum_i v_i^{[\mathcal{C}_l]} = N_{\mathcal{C}_l}$.

By inserting the estimates of equation (11) in equation (8) we get that the steady state cooperative growth rate is

$$g_{\mathcal{C}_l} = (\lambda_{\mathcal{C}_l} - 1) + \langle x^{[\mathcal{C}_l]} \mu \rangle_{\mathcal{C}_l} - \frac{1}{2} \frac{1}{N_{\mathcal{C}_l}} \langle (x^{[\mathcal{C}_l]})^2 \sigma^2 \rangle_{\mathcal{C}_l}, \quad (12)$$

where $x_i^{[\mathcal{C}_l]} = v_i^{[\mathcal{C}_l]} z_i^{[\mathcal{C}_l]}$, is a network centrality index whose relation with the drifts and amplitudes ultimately determines the cooperative growth rate.

C. Determining ESS

To determine the ESS in situations when there is a possibility that unconditional defectors and cooperators may coexist, we consider an alternate-projection method. In particular, notice that the ESS conditions may be reformulated as

$$\begin{aligned} g_i^* &= g_{\mathcal{C}_l}, \quad i \in \mathcal{C}_l, \\ 0 &= (g_{\mathcal{C}_l} - g_i^{\mathcal{D}}) (1 - p_i^*), \end{aligned}$$

resulting in a nonlinear system of $2N$ equations with $2N$ variables (g_i^* and p_i^*) in total. Hence, a simplified, iterative approach based on the alternate projection method can be used for finding the steady state solution. This method may be summarized as follows:

1. Set $p_i^* = 0$ and $g_i^* = g_i^{\mathcal{D}}$ for all i not satisfying the condition (5). Set $p_i^* = 1$ for the remaining entities. To estimate their growth rate solve Eq. (12) for each component of cooperators \mathcal{C}_l and set for each $i \in \mathcal{C}_l$, $g_i = g_{\mathcal{C}_l}$.
2. For all i satisfying $g_i^* < g_i^{\mathcal{D}}$ in the obtained solution, set $p_i^* = 0$ and $g_i^* = g_i^{\mathcal{D}}$. For each remaining component of cooperators, solve again the corresponding growth rate.
3. Repeat steps 1. and 2. until there are no $g_i^* < g_i^{\mathcal{D}}$.

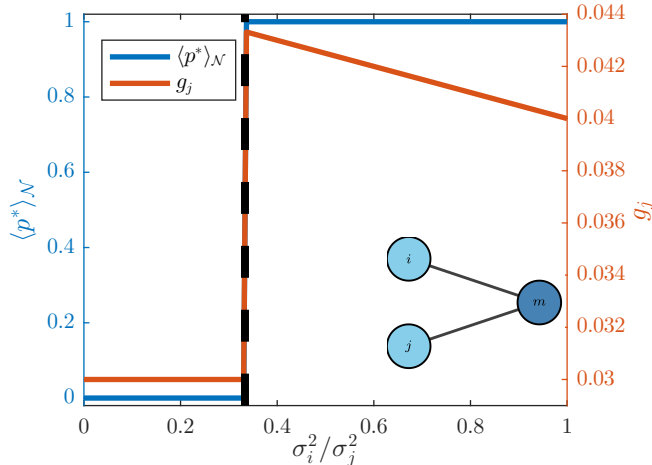


FIG. 2: **Example 1.** Average fraction of unconditional cooperators $\langle p^* \rangle_{\mathcal{N}}$ and steady state growth rate g_j of entity j as a function of the noise amplitude ratio σ_i^2/σ_j^2 . The dashed line is the threshold after which cooperation is evolutionary stable. The inset plot depicts the interaction structure.

D. Simple examples

To provide an illustrative representation for the evolutionary properties of the model in what follows we study three simple examples. The purpose of the first example is to show the evolutionary dynamics in the simplest population structure consisting of only two entities. The second example extends the population size to an arbitrary size of N entities. The last example shows how non-linearities in the cooperative growth rate can arise even in an ordinary interaction structure.

a. Example 1: The first situation that we consider is a replication of the example studied in Ref. [8]. Concretely, we assume an interaction structure of two entities i and j who have the option to share their resources through one pool m , as illustrated in the inset of Fig. 2.

For simplicity, we are going to assume that i has a larger individual steady state growth rate, (i.e. $g_i^{\mathcal{D}} > g_j^{\mathcal{D}}$ and examine the situation from the point of view of entity i . In this case,

the payoff matrix for i reads

$$\begin{array}{cc}
 & j \\
 & C \qquad D \\
 i \begin{array}{c} C \\ D \end{array} & \begin{array}{|c|c|} \hline \langle \mu \rangle_{\mathcal{N}} - \frac{\langle \sigma^2 \rangle_{\mathcal{N}}}{4} & 0 \\ \hline \mu_i - \frac{\sigma_i^2}{2} & \mu_i - \frac{\sigma_i^2}{2} \\ \hline \end{array}
 \end{array} \tag{13}$$

which, after some reordering, implies that full cooperation is ESS if

$$\mu_j - \frac{\sigma_j^2}{4} > \mu_i - \frac{3\sigma_i^2}{4}.$$

In the special case when $\mu_j = \mu_i$, the condition reduces to $3\sigma_i > \sigma_j$. This result is displayed in Fig. 2 where we plot the average steady state incentives for cooperation within the population and the steady state growth g_j of individual j as a function of the square of the amplitude ratio σ_i/σ_j . We observe that at the critical point at $\sigma_i^2/\sigma_j^2 = 1/3$ the growth rate of entity j is largest and afterwards it is decreasing linearly due to the increase in the noise amplitude σ_i of entity i .

b. Example 2: The second example extends the interaction to an arbitrary number of N entities, as depicted in the inset of Fig. 3. This is the well-mixed situation which has been extensively utilized for determining the performance of a particular mechanism in the evolution of cooperation.

To ease the analysis, we assume that a fraction of the population has an individual growth rate larger than $g^{[N]}$ and therefore the individuals belonging to this group behave as defectors. The other fraction, γ , has an equal drift μ and noise amplitude σ .

As a consequence, in this example there is only one component of possible cooperators \mathcal{C} and for each individual i in it we have that $v_i^{\mathcal{C}} = 1$ and $z_i^{[\mathcal{C}]} = \lambda_{\mathcal{C}} = \gamma$. Hence, the cooperative growth rate of this component is

$$g^{\mathcal{C}} = \gamma - 1 + \gamma\mu - \gamma\frac{\sigma^2}{2N}. \tag{14}$$

Clearly, under evolutionary dynamics unconditional cooperation by the entities in the potential cooperator set will be favored only if

$$g^{\mathcal{C}} > \mu - \frac{\sigma^2}{2},$$

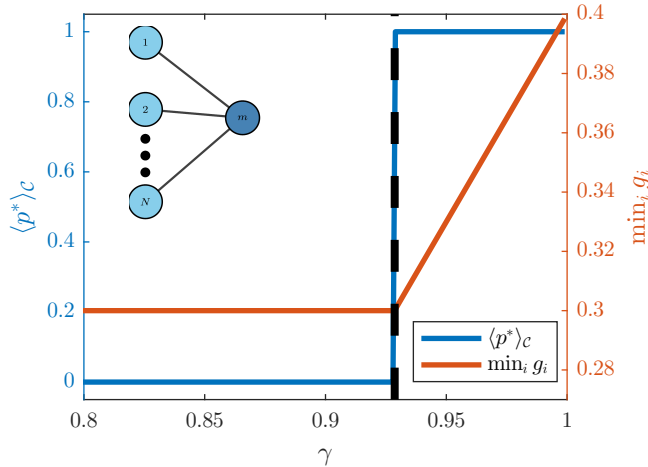


FIG. 3: **Example 2.** Average fraction of unconditional cooperators $\langle p^* \rangle_{\mathcal{C}}$ and minimum steady state growth rate for the entities in the cooperator set \mathcal{C} as a function of the fraction of population belonging to that set γ . The dashed line is the threshold for cooperation to be ESS among the entities in \mathcal{C} , whereas the inset plot describes the interactions. In this case $N = 1000$, $\mu = 0.4$ and $\sigma^2 = 0.2$.

which, when rearranged in terms of γ , yields

$$\gamma > \frac{1 + \mu - \frac{\sigma^2}{2}}{1 + \mu - \frac{\sigma^2}{2N}}. \quad (15)$$

Fig. 3 visualizes the dependence of the minimum steady state growth rate of the potential cooperators as a function of the fraction of potential cooperators γ . It is easily noticed that after condition (15) is satisfied, the growth rate of the entities in the set \mathcal{C} increases, which means that cooperation is an ESS for them.

c. Example 3: In the last example we once more examine a structure consisting of N entities which now interact through 2 pools, m and n . A fixed number of entities $N - 2$ interact solely through pool m and one entity, j , interacts only through pool n . In addition, there is one entity, i , which connects the network by pooling its resources in both m and n . This interaction structure is described in the inset of Fig. 4.

We assume that j has large enough growth rate to behave as defector, and thus study the circumstances under which the remaining $N_{\mathcal{C}} = N - 1$ entities behave as cooperators \mathcal{C} . In

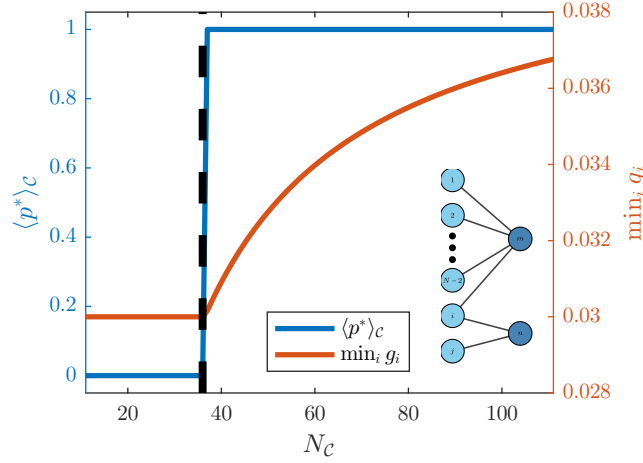


FIG. 4: **Example 3.** Average fraction of unconditional cooperators $\langle p^* \rangle_{\mathcal{C}}$ and minimum steady state growth rate for the individuals in the cooperator set \mathcal{C} as a function of the number of individuals in that set. The dashed line is the threshold for cooperation to be ESS among the individuals in \mathcal{C} , whereas the inset plot describes the interactions. In this example $\mu = 0.04$ and $\sigma^2 = 0.02$.

this case the interaction matrix reads

$$\mathbf{A}_{\mathcal{C}} = \begin{bmatrix} \frac{1}{N_{\mathcal{C}}} & \frac{1}{N_{\mathcal{C}}} & \cdots & \frac{1}{N_{\mathcal{C}}} & \frac{1}{2N_{\mathcal{C}}} \\ \vdots & \vdots & & \vdots & \vdots \\ \frac{1}{N_{\mathcal{C}}} & \frac{1}{N_{\mathcal{C}}} & \cdots & \frac{1}{N_{\mathcal{C}}} & \frac{1}{2N_{\mathcal{C}}} \\ \frac{1}{N_{\mathcal{C}}} & \frac{1}{N_{\mathcal{C}}} & \cdots & \frac{1}{N_{\mathcal{C}}} & \frac{1}{2N_{\mathcal{C}}} + \frac{1}{4} \end{bmatrix}.$$

Moreover, the largest eigenvalue of $\mathbf{A}_{\mathcal{C}}$ is

$$\lambda_{\mathcal{C}} = \frac{\sqrt{9N_{\mathcal{C}}^2 - 4N_{\mathcal{C}} + 4} + 5N_{\mathcal{C}} - 2}{8N_{\mathcal{C}}},$$

with corresponding right-eigenvector entries

$$v_k^{[\mathcal{C}]} = \begin{cases} \frac{N_{\mathcal{C}}}{N_{\mathcal{C}}\lambda_{\mathcal{C}} - \frac{N_{\mathcal{C}}+2}{4} + 1} & \text{if } k = i, \\ \frac{N_{\mathcal{C}} - v_i^{[\mathcal{C}]}}{N_{\mathcal{C}} - 1}, & \text{otherwise,} \end{cases} \quad (16)$$

and $z^{[\mathcal{C}]}$ index entries

$$z_k^{[\mathcal{C}]} = \begin{cases} 3/4 & \text{if } k = i, \\ 1, & \text{otherwise.} \end{cases} \quad (17)$$

To simplify the analysis, we set each entity $k \neq j$ a growth rate $\mu_k = \mu$ and noise amplitude $\sigma_k = \frac{\sigma}{\sqrt{x_k^{[C]}}}$. This leads to a cooperator growth rate

$$g^C = (\lambda_C - 1) + \lambda_C \mu - \lambda_C \frac{1}{2N_C} \sigma^2. \quad (18)$$

On the other hand, the growth rate of each entity when everyone behaves as a defector is

$$g_k^D = \mu - \frac{\sigma^2}{x_k^{[C]}}. \quad (19)$$

Obviously, cooperation will be ESS when $g_C > g_i^D$, which using Eqs. (16-19), can be rewritten in terms of the largest eigenvalue as

$$\lambda_C > \frac{1 + \mu + \frac{\sigma^2}{2N_C} \frac{N_C + 2}{3} - \frac{2\sigma^2}{3N_C}}{1 + \mu - \frac{\sigma^2}{2N_C} + \frac{2\sigma^2}{3}}. \quad (20)$$

We point out that λ_C is a function dependent only on the number of cooperators N_C . Therefore, to numerically examine our derivations in Fig. 4 we display the growth rate of the entities in the set \mathcal{C} as a function of their cardinality. We observe that once unconditional cooperation is achieved by the entities in \mathcal{C} the addition of new entities affects non-linearly the observed time-average growth rate. This serves as an intuitive example that the interaction structure may have a disproportionate effect on the observed cooperative behavior.

E. Random graphs

In a more general, random graph structure, besides the size of the defector set, the positioning of the entities in the network also determines the ESS for each other individual. While equation (8) and the alternate projection method give the solution for the level of cooperation in any arbitrary situation, the extent to which different random graphs are able to support cooperation when defectors are present can not be easily deduced from them.

To provide an insight on this phenomena, here we consider four different types of random graph models i) Random d -regular (RR) graph [17], ii) Erdos-Renyi (ER) random graph [18], iii) Watts-Strogatz (WS) random graph [19], and iv) Barabasi-Albert (BA) random scale-free network [20] and study their robustness in the presence of arbitrary defectors. In an RR graph each entity is characterized with the same degree d , whereas in an ER graph two entities share an edge with probability d/N . Both types of random graphs yield homogeneous

degree distributions and low clustering coefficients. The WS random graph, on the other hand is an extension of the two aforementioned graphs which is able to capture higher levels of clustering. In fact, this random graph type lies in-between the ER and RR graph as its creation starts with an initial structure of an RR and then each edge is re-wired with a fixed probability. Finally, the BA graph is constructed through a preferential attachment mechanism for generating random graphs. As such it yields a power law degree distribution coupled with high clustering.

We point out that each of the studied graph is in fact a monopartite graph. As a consequence it may not be appropriate for a numerical validation of our model. Nevertheless, each monopartite graph can be mapped into a bipartite by considering a replacement graph procedure. In this representation each node behaves as both an individual entity and a pool through which resources are shared [13]. This, coupled with the computationally inexpensive algorithms for the generation of the four random graphs, allows for an easy comparison of their performance.

To assess the robustness of the types of random graphs we conduct the following experiment. We begin by generating a random graph through the typical algorithms that are used for this procedure. Afterwards, we choose a random fraction $1 - \gamma$ of the population. We set the growth rate of the individuals in it to be large enough so as they behave as defectors and characterize the individuals in the other set, the potential cooperators, with an equal drift μ and noise amplitude σ . Under these circumstance, we estimate the steady state growth rates of each individual i belonging to the cooperative cluster \mathcal{C}_l as

$$\begin{aligned} g^{\mathcal{C}_l} &= (\lambda_{\mathcal{C}_l} - 1) + \mu \langle x^{[\mathcal{C}_l]} \rangle_{\mathcal{C}_l} - \frac{\sigma^2}{2N_{\mathcal{C}_l}} \langle (x^{[\mathcal{C}_l]})^2 \rangle_{\mathcal{C}_l} \\ &= (\mu + 1) \lambda_{\mathcal{C}_l} - \frac{\sigma^2}{2N_{\mathcal{C}_l}} \langle (x^{[\mathcal{C}_l]})^2 \rangle_{\mathcal{C}_l} - 1, \end{aligned} \quad (21)$$

and gather the average number of cooperators among the individuals in the potential cooperator set, $\langle p^* \rangle_{\mathcal{C}}$. To get the typical behavior of a particular random graph we average across random graph instances and across defector selection samples.

Numerical results are summarized in Fig. 5a where we plot the average p_i^* among the individuals in the cooperator set as a function of γ . We observe that for small γ the BA graph presents itself as the most supportive for cooperation as it requires the lowest amount of individuals in the cooperator set for some cooperation to exist. It is followed by the ER

and WS graphs, while under this criterion the RR graph is the least robust random graph. Interestingly, when we consider the threshold for full cooperation we get the opposite result, i.e. the RR graph is the most robust random graph, followed by the ER and WS graphs. In this case, the BA graph is the least robust to an invasion of defectors.

The reason for this behavior becomes apparent if we look at the evolution of λ_C and $\langle (x^{[C_i]})^2 \rangle_{C_i}$ as a function of the fraction of individuals belonging in the potential cooperator set. For small γ we observe that there are only slight differences between the four networks, with the ER and BA graph exhibiting larger values for both variables. Since $\mu > \sigma^2$ in this case λ_C decisive in the determination for the level of cooperation, and the networks with a larger eigenvalue will be better promoters of cooperation. As γ increases, the differences in $\langle (x^{[C_i]})^2 \rangle_{C_i}$ become apparent, whereas λ_C converges to the same value for each network. Because $\langle (x^{[C_i]})^2 \rangle_{C_i}$ is related to the amplitude of the noise, the networks with lower value will be better promoters of cooperation. As depicted in Fig. 5c, the RR graph is on average less affected by this condition, i.e. it is more robust to an invasion of defectors.

IV. GENERALIZED RECIPROCITY

So far, we addressed evolutionary behavior in which pooling and sharing is the sole cooperative mechanism. We showed that, as a consequence of the non-ergodicity, if certain conditions are satisfied, cooperation can be evolutionary stable even without the presence of any additional decision making mechanisms. In fact, the presence of additional auxiliary mechanisms should yield dynamics that at least complement the evolution of cooperation. To provide an initial insight on the role of these mechanisms, here we examine the cooperative behavior in the presence of a state-based generalized reciprocity update rule.

Generalized reciprocity suggests that cooperation can emerge as a consequence of previous positive experience with not necessarily the same group of opponents, i.e. it is based on the rule of “help anyone if helped by someone”. This is significantly different from the two main forms of reciprocity, direct and indirect, which explain the emergence of cooperation either as a result of repeated encounters between the same group of individuals or as an attempt to build positive reputation for future interactions [21, 22].

The main presumption which favors generalized reciprocity over other reciprocal mech-

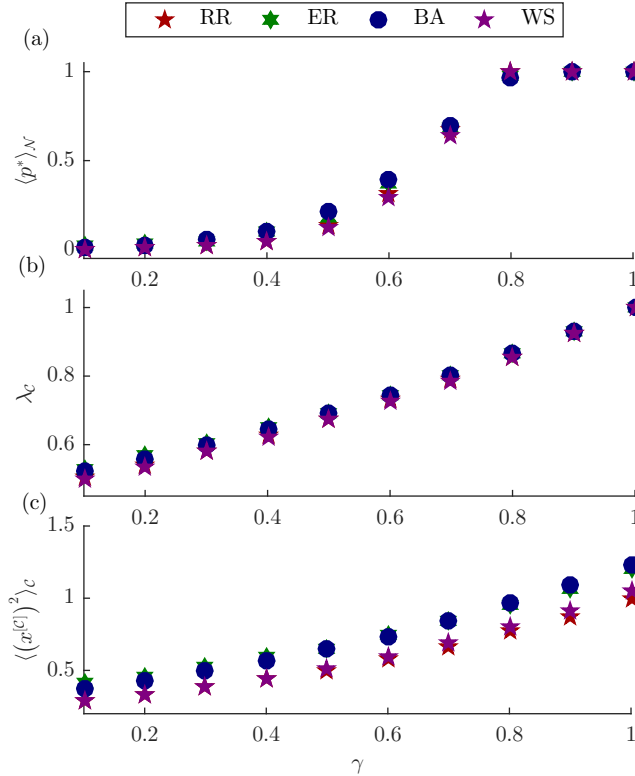


FIG. 5: **The role of complex networks in heterogeneous populations.** (a) Average steady state incentive for cooperation $\langle p^* \rangle_c$ as a function of the fraction of potential cooperators γ for RR, ER BA and WS graphs. (b) Average largest eigenvalue λ_c of the matrix A_C as a function of γ for the same networks. (c) Average $\langle (x^{[C_i]})^2 \rangle_c$ as a function of γ . (a-c) In the simulation $\mu = 0.5$ and $\sigma^2 = 0.8$. The results are averaged across 100 defector realizations and 100 graph realizations each graph each having 10 nodes and an average degree of 4.

anisms is that individuals following this rule can be said to exhibit a simple state-based behavior. Due to this straightforward decision making rule, generalized reciprocity has been observed in a wide range of animal and human societies each manifesting different level of cognitive prowess and interacting in various environments [23–27].

While the extent to which generalized reciprocity is able to evolve as a sole cooperation mechanism has been a subject to an active debate, recent studies have shown that once this mechanism is present in a system, it induces dynamics which assist the stability of cooperation [28–32]. Concretely, in [33, 34] it was argued that state-based generalized reciprocity

effectively prevents individuals from being exploited by defectors, whereas in [3] it was suggested that this prevention is accompanied with maximization of the level of cooperation displayed by each individual. Nevertheless, the theoretical work done so far has assumed that individuals interact in an additive environment where ensemble averages are a good approximation for the stochastic behavior of each individual. In this section we extend the rule to account for possible multiplicative resource dynamics.

A. Decision making rule

To study the individual behavior under a simple generalized reciprocity rule we consider an update based on the individual estimate of the growth rate of entity i

$$p_i(t + \Delta t) = f_{i,t}[g_i(y_i(t), t)], \quad (22)$$

where $f_{i,t} : \mathbb{R} \rightarrow [0, 1]$ is monotonic (nondecreasing). A plausible choice would be the sigmoid (logistic) function

$$f_{i,t}(\omega) = [1 + \exp\{-\kappa_i(t)(\omega - \omega_i)\}]^{-1}, \quad (23)$$

where the midpoint ω_i is given by the steady state of $g_i(y_i(t), t)$ without pooling, i.e., $g_i^{\mathcal{D}}$.

We remark that we purposefully allow for the steepness of the sigmoid function to be an unbounded monotonically increasing function of t , so as to account for the time-dependence in the variance of $g_i(y_i(t), t)$. For simplicity, we focus on the special case when $\kappa(t) = t^\alpha$ where α is a positive parameter that captures the learning rate of the entities. In particular, $\alpha < 1$ corresponds to convergence towards equilibrium incentives to cooperate at a rate lower than the elapsed time t , whereas $\alpha > 1$ provides the opposite dynamics.

We point out that the introduced rule provides a simple description for the cooperative behavior in a wide range of interaction structures. The advantage of the behavioral update lies in its simplicity since (22) implies that an entity only has to know its current amount of resources in order to determine the next action. This is significantly different from other decision making rules where entities are required to optimize over domains depending on both opponent behavior and possible future interactions [35].

B. Model properties

In the analysis performed in Section III we always ended up with dynamics that have a steady state. However, the introduction of the state-based generalized reciprocity rule may in fact disturb this property of the model and we may end up with complex dynamics whose study is out of the scope of the paper.

To greatly ease the analysis of the generalized reciprocity here we consider two situations. In the first situation, we examine the individual cooperative behavior under the assumption that there is a steady state growth rate g_i^* for every entity i . In the second situation, we study the properties of the model numerically and derive an analytical solution for the model in the circumstance when $\alpha < 1$ since, as it will be shown, there is always a steady state.

a. Cooperative behavior: Let us assume that there is a steady state cooperative behavior p_i^* and growth rate g_i^* for each entity i conforming to the rule (22). In addition, we assume that the growth rate of each entity is set such that the system is non-degenerate. By non-degenerate we mean that $g_i^{\mathcal{D}} \neq g^{\mathcal{C}}$ for all i . Then, we can derive the following properties of the model

i. Prevention of exploitation: – It can be easily shown that $g_i^* < g_i^{\mathcal{D}}$ is an impossible situation for any entity following the behavioral update rule. To see this, assume that entity i follows (22) and has $g_i^* < g_i^{\mathcal{D}}$. Then, the behavioral update rule indicates that the steady state incentive for cooperation of this entity is $p_i^* = 0$. Subsequently, this implies that

$$y_i(t + \Delta t) \geq y_i(t) \left[1 + \mu_i \Delta t + \sigma_i \varepsilon_i(t) \sqrt{\Delta t} \right]. \quad (24)$$

Taking the limit as $t \rightarrow \infty$ we get that $g_i^* \geq g_i^{\mathcal{D}}$, thus contradicting our initial assumption. This is a favorable property of state-based generalized reciprocity which has been also observed in additive dynamics [33]. It significantly differs from other forms of generalized reciprocity since it has been shown that they are prone to exploitation [31].

ii. Sufficient condition for existence of unconditional cooperators: – The behavioral update rule coupled with the monotonicity and unboundedness of $\kappa_i(t)$ imply that if $g_i^* > g_i^{\mathcal{D}}$ then $p_i^* = 1$. Moreover, it follows that a necessary condition for $p_i^* < 1$ is $g_i^* = g_i^{\mathcal{D}}$.

Altogether, in steady state the entities may thus be attributed to two (disjoint) sets, $\mathcal{D}_{gen} = \{d \in \mathcal{N} : p_d^* < 1\}$ and $\mathcal{C}_{gen} = \{c \in \mathcal{N} : p_c^* = 1\}$, depending on the steady incentive for cooperation p_i^* . The entities in \mathcal{D}_{gen} are further characterized by $g_d^* = g_d^{\mathcal{D}}$, while the entities y_c in \mathcal{C}_{gen} have an unknown growth rate $g_c \geq g_c^{\mathcal{D}}$, which is dependent on the network parameters. We will refer to the entities in the sets \mathcal{D}_{gen} and \mathcal{C}_{gen} as “generalized defectors”, respectively “generalized cooperators”, with an intention to emphasize their role in the pooling and sharing mechanism.

b. Numerical experiment: The behavior of the individual growth rates ultimately depends on the magnitude of α . This parameter indicates the speed at which every entity reacts to the environment: if an entity has a smaller-than-expected growth, it will defect faster proportionally with α , and cooperate faster otherwise. Even if the fraction of resources that is pooled and shared is small, the amount may be non-negligible for some of the entities which behave as unconditional defectors in evolutionary sense and, in fact, it may significantly increase their growth rate, thus making them “generalized cooperators”. In other words, while the rule asserts that the entities which experience lower growth than their own eventually end up as generalized defectors, the number of generalized defectors may in general be smaller than the number of defectors inferred through evolutionary stability analysis.

To illustrate this effect we make use of the network given in Fig. 1. Concretely, we initialize the drift and amplitudes of the entities so as under evolutionary analysis $p_3^* = 0$ and cooperation is unstable for every other entity. Then, we simulate the coupled dynamics of equations (1) and (22) for 2×10^4 time steps and record the incentives for cooperation among the individuals in the potential generalized cooperator set at the last point in time.

Fig. 6a provides a boxplot for the incentives for cooperation for each entity. In general, we observe two different regimes depending on α . The first appears when $\alpha < 1$. In this case, the incentive to cooperate p_i for each individual i appears to be at a value less than 1 but larger than 0. As α increases, the incentives to cooperate for each $i \neq 3$ also increase, eventually converging to $p_i = 1$. In contrast, the incentive of entity 3 decreases and converges to $p_3 = 0$. We assert that for the lower values of α the system is not in steady state and is eventually converging to the steady state where $p_i^* = 1$ for all $i \neq 3$, $p_3^* = 0$ and $g_i^* = g_3^{\mathcal{D}}$. This is evidenced in Fig. 6b where we plot the numerically observed growth rate for each

individual as a function of α . Concretely, we notice that the observed growth rate of each $i \neq 3$ is larger than their defector growth rate, thus implying that $p_i^* = 1$. In contrast, the growth rate of 3 is smaller than its defector growth rate. As a consequence, the incentive to cooperate of this entity must be converging to 0. This slow convergence is illustrated in Fig. 6c where we visualize the dynamics over time of each $p_i(t)$ for various α .

The second regime occurs when $\alpha > 1$. In this situation we observe that the incentives for cooperation for each entity i vary from one simulation to another. One explanation for this phenomena is the fact that when $\alpha \geq 1$ the steepness of the logistic curve diverges with a rate that is at least as fast as the divergence of the resources of each entity. This reduces the domain of all $p_i(t)$ to $\{0, 1\}$ faster. Since growth rate of each entity is highly stochastic we may observe non-equilibrium dynamics even though we numerically find that on average the growth rate of each potential generalized cooperator is larger than expected (Fig. 6b).

c. Analytical solution: The general case of $\alpha < 1$ in any interaction structure can be easily analytically solved and thus the observations explained. To see this, let i represent the strongest entity in the network in the sense that $g_i^D > g^C$ and $g_i^D > g_j^D$ for all $j \neq i$. We claim that the limit of the growth of each entity is at least as large as g_i^D . For every finite time t we approximate the growth rate $g_j(t)$ of each entity $j \neq i$ and notice that this quantity is bounded from below by the the growth induced by the shared resources from the strongest entity. Since the defection is slow enough, these shared resources are enough to bring the growth of each $j \neq i$ to g_i^D .

Formally, we have

$$g_j(t + \Delta t) \approx \frac{1}{t + \Delta t} \log \left(y_j(t) (1 - p_j(t)) r_j(t, \Delta t) + \sum_{k \neq i} A_{jk} p_k(t) y_k(t) r_k(t, \Delta t) + A_{ji} p_i(t) y_i(t) r_i(t, \Delta t) \right),$$

where we define $r_n(t, \Delta t) = 1 + \mu_n \Delta t + \sigma_n \varepsilon_n(t) \sqrt{\Delta t}$. Clearly, for fixed t , $r_j(t, \Delta t) \rightarrow 1$ as $\Delta t \rightarrow 0$. Thus each term within the logarithm is positive. This, in turn, implies that

$$\begin{aligned} g_j(t + \Delta t) &\geq \frac{1}{t + 1} \log (A_{ji} p_i(t) y_i(t) r_i(t, \Delta t)) \\ &= \frac{1}{t + 1} \left(\log (A_{ji}) + \log \left(\frac{1}{1 + \exp(-t^\alpha (g_i(t) - g_i^D))} \right) + \log (y_i(t)) + \log (r_i(t, \Delta t)) \right) \\ &\geq \frac{1}{t + 1} \left(\log (A_{ji}) + \log \left(\frac{1}{1 + \exp(ct^\alpha)} \right) + \log (y_i(t)) + \log (r_i(t, \Delta t)) \right), \end{aligned}$$

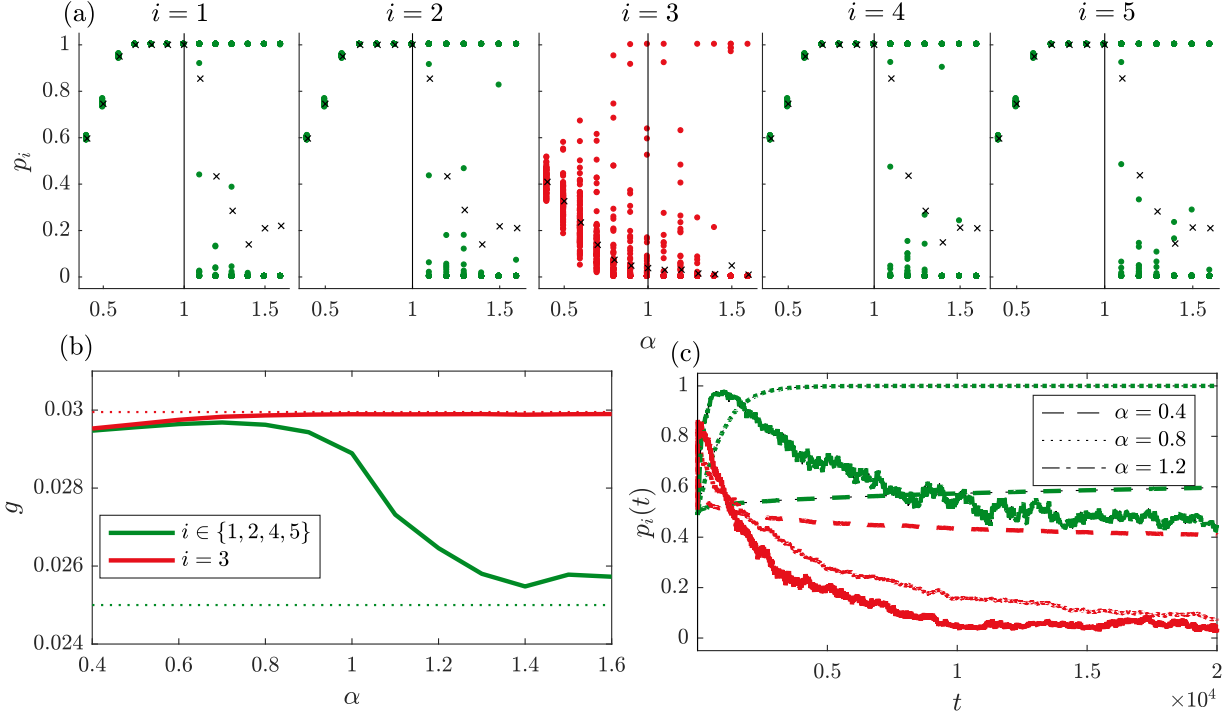


FIG. 6: **State-based generalized reciprocity in multiplicative dynamics.** (a)

Observed incentives for cooperation $p_i(t)$ for each individual at $t = 2 \times 10^4$ over 100 realizations. The circles are the results from each realization, whereas the crosses are the estimated averages across realizations for a given α . (b) Numerically observed growth rate averaged across realizations. (c) Dynamics over time for the average $p_i(t)$ across realizations. The green lines are the averages for individuals $i \in \{1, 2, 4, 5\}$ whereas the red lines are the averages for $i = 3$. (a-c) The parameters are set to $\mu_i = 0.03$ for all i ,

$$\sigma = \sqrt{0.01} \text{ for } i \neq 3 \text{ and } \sigma = 0.01 \text{ for } i = 3.$$

for some constant $c > 0$ as a consequence of the Gronwall-Bellman lemma [36]. In the limit as $t \rightarrow \infty$, the inequality reduces to

$$\begin{aligned} \lim_{t \rightarrow \infty} g_j(t + \Delta t) &\geq \lim_{t \rightarrow \infty} \frac{1}{t+1} \left(\log(A_{ji}) + \overbrace{\log\left(\frac{1}{1 + \exp(ct^\alpha)}\right)}^{\sim_\infty(-ct^\alpha)} + \log(y_i(t)) + \log(r_i(t, \Delta t)) \right) \\ &= \lim_{t \rightarrow \infty} \frac{1}{t+1} \log(y_i(t)) \geq g_i^{\mathcal{D}}. \end{aligned}$$

This leads to the situation where each entity exhibits a growth rate equal to the growth rate of the strongest individual $g_i^{\mathcal{D}}$. In turn, from the cooperative behavior properties *i.* and *ii.*

we infer that $p_j^* = 1$ for all $i \neq j$ and $p_i^* < 1$.

V. CONCLUSION

We investigated the effect of multiplicative resource dynamics on the evolution of cooperation in populations with heterogeneous individual traits. We found out that these dynamics induce evolutionary behavior which may lead to emergence of cooperative components within the population structure. The properties of each component are characterized solely by the interaction topology and the traits possessed by the entities belonging in it. Thus, we may observe great disparities in the owned resources between entities from different components, and yet both of them will coexist.

Moreover, by introducing a simple state-based decision making rule we showed that generalized reciprocity enhances the promotion of cooperation in multiplicative environments. By construction, the decision making rule produces behavior under which entities with observed growth rates at time t that are greater than in the unconditional defector situation, will have greater incentives to cooperate. For the regime in which the learning rate is slower than the temporal dynamics, we analytically derived the exact behavior of each entity. When the learning rate is faster than the temporal dynamics we numerically observed complex behavior. While a detailed study of this behavior is required, we believe that its implications are non-trivial and may hide valuable information on events such as the co-evolution of life cycles and multicellularity [37–39].

The implementation of our results goes beyond explaining the evolution of cooperation. In particular, the introduced rule is directly related to the concept of novelty search where individual entities decide their actions on the basis of previous experience [12]. As such it is omnipresent in reinforcement learning and has been utilized in developing machines that efficiently mimic human behavior. In this aspect, we argue that the results discovered here behave as a building block in constructing machines which interact in a multiplicative environment.

[1] E. Pennisi, *Science* **309**, 93 (2005).

- [2] F. Stollmeier and J. Nagler, *Physical Review Letters* **120**, 058101 (2018).
- [3] V. Stojkoski, Z. Utkovski, L. Basnarkov, and L. Kocarev, *Physical Review E* **97**, 052305 (2018).
- [4] M. A. Nowak, *Science* **314**, 1560 (2006).
- [5] M. Roper, M. J. Dayel, R. E. Pepper, and M. Koehl, *Physical Review Letters* **110**, 228104 (2013).
- [6] G. Yaari and S. Solomon, *The European Physical Journal B* **73**, 625 (2010).
- [7] T. Liebmann, S. Kassberger, and M. Hellmich, *European Journal of Operational Research* **258**, 193 (2017).
- [8] O. Peters and A. Adamou, arXiv preprint arXiv:1506.03414 (2015).
- [9] V. Stojkoski, Z. Utkovski, L. Basnarkov, and L. Kocarev, arXiv preprint arXiv:1901.08950 (2019).
- [10] O. Peters and M. Gell-Mann, *Chaos: An Interdisciplinary Journal of Nonlinear Science* **26**, 023103 (2016).
- [11] M. Taborsky, J. G. Frommen, and C. Riehl, *Philos. Trans. Roy. Soc. B.* **371** (2016).
- [12] J. Lehman and K. O. Stanley, in *ALIFE* (2008) pp. 329–336.
- [13] M. Perc, J. Gómez-Gardeñes, A. Szolnoki, L. M. Floría, and Y. Moreno, *Journal of the royal society interface* **10**, 20120997 (2013).
- [14] F. C. Santos, M. D. Santos, and J. M. Pacheco, *Nature* **454**, 213 (2008).
- [15] B.-E. Sæther and S. Engen, *Trends in ecology & evolution* **30**, 273 (2015).
- [16] M. Perc, J. J. Jordan, D. G. Rand, Z. Wang, S. Boccaletti, and A. Szolnoki, *Physics Reports* **687**, 1 (2017).
- [17] B. Bollobás, *Modern graph theory*, Vol. 184 (Springer Science & Business Media, 2013).
- [18] P. Erdos and A. Rényi, *Publ. Math. Inst. Hung. Acad. Sci* **5**, 17 (1960).
- [19] D. J. Watts and S. H. Strogatz, *Nature* **393**, 440 (1998).
- [20] A.-L. Barabási and R. Albert, *Science* **286**, 509 (1999).
- [21] R. Axelrod and W. D. Hamilton, *Science* **211**, 1390 (1981).
- [22] R. Alexander, *The biology of moral systems* (Routledge, 2017).
- [23] C. Rutte and M. Taborsky, *PLoS Biol* **5**, e196 (2007).
- [24] K. L. Leimgruber, A. F. Ward, J. Widness, M. I. Norton, K. R. Olson, K. Gray, and L. R.

- Santos, PloS one **9**, e87035 (2014).
- [25] N. Gfrerer and M. Taborsky, Sci. Rep. **7** (2017).
- [26] M. Y. Bartlett and D. DeSteno, Psychol. Sci. **17**, 319 (2006).
- [27] L. Stanca, J. Econ. Psychol. **30**, 190 (2009).
- [28] T. Pfeiffer, C. Rutte, T. Killingback, M. Taborsky, and S. Bonhoeffer, Proceedings of the Royal Society of London B: Biological Sciences **272**, 1115 (2005).
- [29] D. J. Rankin and M. Taborsky, Evolution **63**, 1913 (2009).
- [30] G. S. van Doorn and M. Taborsky, Evolution **66**, 651 (2012).
- [31] M. A. Nowak and S. Roch, Proceedings of the Royal Society B: Biological Sciences **274**, 605 (2006).
- [32] T. Ito, R. Suzuki, and T. Arita, Artificial Life and Robotics , 1 (2018).
- [33] Z. Utkovski, V. Stojkoski, L. Basnarkov, and L. Kocarev, Physical Review E **96**, 022315 (2017).
- [34] V. Stojkoski, Z. Utkovski, E. Andre, and L. Kocarev, arXiv preprint arXiv:1805.09101 (2018).
- [35] V. Stojkoski, Z. Utkovski, E. Andre, and L. Kocarev, Physica A: Statistical Mechanics and its Applications , 121805 (2019).
- [36] R. Khasminskii, *Stochastic stability of differential equations*, Vol. 66, Stochastic Modelling and Applied Probability Book Series (Springer Science & Business Media, 2011).
- [37] K. Hammerschmidt, C. J. Rose, B. Kerr, and P. B. Rainey, Nature **515**, 75 (2014).
- [38] P. B. Rainey and B. Kerr, Bioessays **32**, 872 (2010).
- [39] Y. Pichugin, C. S. Gokhale, J. Garcia, A. Traulsen, and P. B. Rainey, Journal of theoretical biology **387**, 144 (2015).